RSC Advances

ROYAL SOCIETY OF CHEMISTRY

www.rsc.org/advances

Interface engineering and efficiency improvement of monolayer graphene-silicon solar cells by inserting an ultra-thin LiF interlayer

Dikai Xu, Xuegong Yu*, Lijian Zuo, Deren Yang

State Key Laboratory of Silicon Materials and Department of Materials Science & Engineering

Zhejiang University, Hangzhou 310027, China

*Corresponding author at: State Key Laboratory of Silicon Materials and Department of Materials Science & Engineering, Zhejiang University, Hangzhou 310027, China 110004

Tel.: 0086 571 87951667

Email address: yuxuegong@zju.edu.cn

Abstract

Graphene (Gr)-Si Schottky junction solar cells have recently attracted intensive attention as a candidate of low-cost photovoltaic devices. However, the efficiency of Gr-Si solar cells still need to be further improved. Here, we have introduced an ultra-thin LiF layer in-between the Si and Aluminum (Al) back electrode of Gr-Si solar cells. It is found that the carrier recombination at the back surface is significantly suppressed, directly resulting in the improvement of external quantum efficiency (EQE) of devices in the long wavelength range of 800-1100 nm. Meanwhile, the back contact resistance is greatly reduced, and therefore the fill factor (*FF*) of devices is greatly improved. As a result, a highest power-conversion-efficiency (PCE) of 6.25% has been obtained for a pristine Gr-Si solar cell, which is further improved to 10.61% after chemical doping. These results

pave a new way to the fabrication of high efficiency Gr-Si solar cell.

KEYWORDS: solar cells; Graphene; back contact; carrier recombination

1. Introduction

Tremendous interesting has been focused on photovoltaic (PV) electricity based on solar cells as power sources due to the worldwide energy issue. The mostly used commercial solar cells are fabricated by Si material since it is earth-abundant, stable and suitable for photovoltaic industry. However, the fabrication of traditional crystalline Si solar cells is complicated, based on the formation of a p-n junction. Compared to p-n junction, Schottky junction solar cells have merits of low-cost and easy-to-fabricated. However, the thick metal layer usually used for the formation of Schottky junction with Si has poor transparency, which limits the sunlight absorption of solar cells. Therefore, in the past few years transparent carbon nanotube (CNT) films have been used to form solar cells with Si, which yields a power-conversion-efficiency (PCE) of 10-15%.[1-4] Graphene (Gr), as a fascinating two-dimensional (2D) material with high transparency, high conductivity and unique quantum properties, has triggered great research enthusiasm in PV application. [5-8] Since the first Gr-Si solar cell achieved a PCE of 1.5%, many efforts have been employed to improve the solar cell efficiency by different routes. [9] It has been widely accepted that the PCE of Gr-Si Schottky solar cells can be improved by increasing the electrical conductivity of Gr film with chemical or electrical field doping which results in the highest efficiency of 8.9%. If combined with the application of antireflective film, the efficiency of a chemically doped Gr-Si solar cell can reach 14.5%.[10] However, the chemical doping is usually not stable and the corresponding Gr-Si solar cell has to suffer the efficiency degradation. For the pristine Gr-Si solar

cell, the difficulty in its efficiency improvement originates from the interface recombination of carriers, including the front and back surfaces. Recently, a chemical-doping-free Gr-Si solar cell with a record PCE of 6.18% was obtained by insert a Graphene oxide (GO) interlayer between Si and Gr to suppress the front surface recombination of solar cells reported by our group.[11] In order to further improve the performance of Gr-Si solar cells, it is necessary to reduce the recombination at the backside of Gr-Si solar cells.

Here, we have introduced a lithium fluoride (LiF) layer with nominal thickness of 0.5 nm in-between the Si and Al back electrode to suppress the back surface recombination of Gr-Si solar cells. The external quantum efficiency (EQE) of solar cells is significantly improved and meanwhile, the dark current and the back contact resistance decrease. A PCE up to 6.25% can be obtained for the pristine Gr-Si solar cell. This value can be further improved to 10.61% after HNO_3 chemical doping. To our best understanding, such efficiencies are the record values for the pristine and chemically-doped Gr-Si solar cells without the application of antireflection layer. [10]

2. Experimental

A. Graphene preparation

The large-area monolayer Gr films were grown on a copper foil by a low pressure chemical vapor deposition (LPCVD) method at 1000 ^{o}C using CH_4 (20 sccm) as carbon source and H_2 (40 sccm) as reduction gas. The sheet resistances of Gr films are in the range of 400~1000 Ω/sq determined by a four probe method. A well-defined

Polymethylmethacrylate (PMMA) assisted wet transfer process was used for Graphene transfer.[12] Briefly speaking, the graphene was spin-coated with PMMA in Ethyl lactate. The PMMA was dried on a hot plate at 150 ^{o}C for 15 min. The Gr on the backside of Cu foil was etched away by ultraviolent ozone cleaning process for 10 min. After that, the underlying Cu foil was etched by aqueous ammonium persulfate ($(NH_4)_2S_2O_8$, Aladdin®) solution (1 M). The resultant Gr films were cleaned by deionized water for several times.

B. Device fabrication

N-type <100> c-Si wafer (1.2×1.2 cm^2, resistivity 1-10 Ω/cm and thickness 300 μm) to construct Gr-Si Schottky junction solar cells. The Si substrates were firstly soaked in a diluted HF solution for several minutes to remove the native SiO_2, and then rinsed by deionized water followed by N_2 gas drying. The cleaned Si substrates were set for about 2 hours permitting a thin native SiO_2 passivation layer to grow. The PMMA-supported Gr films were directly transferred onto the Si substrates. After drying at room temperature, residual PMMA on the Gr films was removed by annealing at 400 ^{o}C for 1 h in N_2 atmosphere. Ag paste was coated along the outline of Gr films. The device active area was determined by black tapes in the range of 0.12~0.18 mm^2. the Ag paste and the outside area was completely covered. A 0.5 nm thick LiF layer and a 150 nm thick Al layer were successively thermal deposited on the back-side of Si substrate as back contact for devices. Thickness of LiF layer was determined by a film thickness meter (INFICON, SQM-160). The schematic diagram

of device structure is shown in Figure 1(a). Reference solar cells without the LiF interlayer were fabricated in the same way. Furthermore, HNO_3 doping process was carried out by exposing Gr films to HNO_3 fumes for 1 min. Note the Ag electrodes gradually turned yellow during a prolong HNO_3 doping process. The doping process should be carefully controlled to avoid severe oxidation of Ag front electrodes.

The performance of solar cells were measured by a Keithley 2400 source meter and a solar simulator (94022A, Newport®) under AM 1.5G conditions at an illumination intensity of 100 mW/cm^2, calibrated by a standard Si solar cell (PVM937, Newport®). The external quantum efficiency (EQE) of solar cells was measured by an EQE measurement system (QEX10, PV Measurements, Inc.) across a wavelength range of 400-1100 nm.

3. Results and discussion

Figure 1(b) shows the Raman spectrum of a Gr film. A very weak D peak at ~1350 cm^{-1} indicates that the Gr film is high quality. The intensity ratio of 2D and G peak is 2.2, suggesting that the Gr film is monolayer. Figure 2 shows the Scanning Electron Microscopy (SEM) image of nominally 0.5 nm thick LiF layer deposited on the Si wafer. The as-grown LiF layer is formed by close-packed flakes with diameters around 20 nm. Since the deposited LiF layers are not very uniform, all the thickness of LiF interlayer mentioned in following part are nominal thickness.

Figure 3(a) displays the current density-voltage (*J-V*) curves of our best Graphene-Si solar cell with and without a LiF interlayer under AM 1.5G conditions

illumination at 100 mW/cm^2. Meanwhile, the photovoltaic parameters of solar cells with and without LiF interlayer, including short-circuit current density (J_{SC}), open-circuit voltage (V_{OC}), fill factor (*FF*) and PCE are summarized in Table 1. It is noteworthy that an obvious increase in V_{OC} for the solar cells with a LiF interlayer can be observed, whose maximum value is up to ~424 mV. The J_{SC} for the devices with and without LiF was in range of 24.83~27.18 mA/cm^2 and 21.39~26.59 mA/cm^2, respectively. The values of *FF* for the reference cells were in range of 44.21%~52.25%, which increased to 52.78%~54.50% for the solar cells with a LiF interlayer. As a result, the PCE of devices increased from 3.81%~4.67% to 5.48%~6.25% after the application of LiF interlayers. Such high efficiency, for our solar cell with a LiF interlayer is comparable or even higher than those for Gr-GO-Si MIS solar cells reported by Yang *et al*, which is the current record of Gr-Si Schottky solar cell without chemical doping.[11] After the HNO_3 doping process, the V_{OC}, J_{SC}, *FF* and PCE of the Gr-Si solar cell with a LiF interlayer were dramatically improved to 540 mV, 29.07 mA/cm^2, 67.54% and 10.61%, respectively. To our best understanding, this efficiency is the highest value for Gr-Si Schottky solar cells without antireflection to date.

Figure 3(b) compares the EQE spectra of Gr-Si solar cells with and without a LiF interlayer. It is clearly seen that the EQE of device with a LiF interlayer in long wavelength (800~1100 nm) was significantly improved. The integrated current densities for the devices with and without a LiF interlayer were 26.26 mA/cm^2 and 24.66 mA/cm^2, respectively, which are consistent with the J_{SC} improvement observed

in *J-V* curves. It should be noted that the EQE of the Gr-Si solar cell with a LiF interlayer has a highest value of ~65% in range of 750~850 nm, which is in agreement with the reflectivity rate of Si.[13, 14] It indicates that our solar cell has high carrier collection efficiency.

To take an insight into the improvement provided by the LiF interlayer, we compare the *J-V* curves of Gr-Si solar cells with and without a LiF interlayer under dark condition, as shown in Figure 3(c). The reversed saturation current (J_s) can be extracted by fitting the *J-V* curves based on the thermionic emission model as follows,

$$J = J_s\left[\exp(\frac{qV}{nkT}) - 1\right] \quad (1)$$

where J is the current density, V the applied voltage, T the absolute temperature, k the Boltzmann constant and q the electronic charge. The J_s of devices with a LiF interlayer was 2.50×10^{-4} mA/cm^2, which is one order of magnitude lower than that of devices without a LiF interlayer, 6.34×10^{-3} mA/cm^2. It indicates that the carrier recombination is significantly suppressed due to the introduction of a LiF interlayer. Figure 3(d) shows the dV/d(ln$J$) versus J curves for the solar cells with and without a LiF interlayer. The series contact (R_s) of devices were extracted from the dV/d(ln$J$) versus J curves (see details in ESI) .[15, 16] It can be seen that the values of R_s for the devices with a LiF interlayer are in the range of 0.80~0.92 Ω cm^2, while those for the devices without a LiF interlayer are in the range of 0.93~2.43 Ω cm^2. The reduction in R_s will improve the *FF* of devices.

Figure 4 compares the contact resistances between Al and n-Si before and after introducing the LiF interlayer, based on the transmission line measurement (TLM)

method.[17] It can be seen that the resistance is 10.5 Ω for the direct Al/Si contact and 3.49 Ω for the Al/LiF/Si contact, respectively. Further calculation (see details in ESI) indicates that the contact resistance decreases from 1.9×10^{-1} Ω cm^2 to 6.3×10^{-2} Ω cm^2, due to the introduction of a LiF interlayer.

In principle, the reduction of carrier recombination leads to improvement of EQE. Long wavelength photons tend to be absorbed in deep region of the Si substrate. In the Gr-Si solar cells, holes generated in such deep region can easily migrate towards the back surface where carrier recombination takes place. [18] Therefore, we argue the observed higher EQE in long wavelength can be ascribed to less recombination and more efficient electron collection at the back surface of solar cells.

Based on the analysis of the *J-V*, EQE and contact resistance data for the samples with and without LiF interlayer, we propose the LiF interlayer has beneficial effects on band alignment of Gr-Si solar cells (Figure 5). It is well-accepted that a Schottky barrier always exists in the case of metal directly contacting with Si, due to Fermi level pinning by interface states. For Al/n-Si Schottky junction, the potential barrier height (ϕ_B) was reported to be ~0.5 eV.[19] In this case, the electrons need to cross through such an energy barrier to be collected by Al back electrode and therefore reduce the electron current (see the red solid line in Figure 5(a)). However, these holes will increase the recombination probability of electron current. As a result, the decrease of current and the drop of EQE in long wavelength range occur for the reference Gr-Si solar cell, which are consistent with our observation. In the presence of LiF ultra-thin interlayer (see Figure 5(b)), the inserted LiF can dramatically reduce

the work function of Al to about 3.3 eV,[20] due to existence of a large dipole moment.[21] This finally reduces the Schottky barrier between Al and Si. In some extreme cases, the large work function difference generates band bending towards opposite direction, which could repel the holes back and therefore reduce the carrier recombination.[16] The suppressed recombination and enhanced holes blocking effect should lead to improvement of J_{SC}, V_{OC} of devices. It should be noted that the LiF in this experiment, as an insulator, is thin enough for electron to tunnel through. Therefore, the reduction in contact resistance, as well as series resistance of Gr-Si solar cells, can be ascribed to the lowering of Al work function by introduction of LiF, which have been widely observed in OLED[20-23] and OPV[24, 25] devices.

The adjustment of band alignment of Gr-Si Schottky solar cells offered by the LiF interlayer could help explain the improvement of J_{sc}, V_{oc}, FF of devices. We should mention that the optimal thickness of LiF interlayer reported in photovoltaic devices was in range of 0.5~1.2 nm.[26-29] However, in our experiments, the value 0.5 nm is preferred. We compare six Gr-Si solar cells in the same batch with 0.5 and 1.2 nm thick LiF interlayer. Relatively poorer performance for devices with a 1.2 nm LiF interlayer is obtained (see *J-V* characteristics under illumination shown in Figure S2(a) and the photovoltaic parameters of all the six devices summarized in Table S1). We notice that the J_{SC} of solar cells with different thickness are almost identical, which is consistent with EQE spectrum (see Figure S2(b)). The electron transport could become more difficult for a thicker LiF interlayer. Therefore, lower *FF* can be obtained for solar cells with a thicker LiF interlayer, leading to poorer photovoltaic

performance.

Here, special attention has been placed on the stability of Gr-Si solar cell with a LiF interlay after storing for several days. Table S2 summarizes the evolution of the photovoltaic parameters for pristine Gr-Si solar cells with LiF interlayer during the storing time. A dramatic increasing of V_{OC} and PCE is obtained after one day storing, which can be attributed to the nature doping effect induced by O_2 and H_2O absorbed on annealed Gr films. [30, 31] After that, performance of devices almost keeps constant in one week, indicating that the Gr-Si solar cells with a LiF interlayer has a good stability. However, the performance of HNO_3 doped Gr-Si solar cells degrades rapidly, which is consistent reported previously.[32] Much more efforts should be paid on developing stable doping method for Gr films.

4. Conclusions

In summary, we have introduced a LiF ultra-thin interlayer between Si and Al back contact to improve the performance of Gr-Si Schottky junction solar cells. High PCE of 6.25% and 10.61% for pristine and chemically-doped Gr-Si solar cell have been achieved, respectively. The improved performance was ascribed to the reduction in carrier barrier height, recombination, and contact resistance at the backside of solar cell. Such device architecture has potential to be further developed if antireflection techniques and multilayer Gr are applied. These results pave a new way to the fabrication of high efficiency Gr-Si solar cell, which is interesting for low-cost photovoltaics.

Acknowledgements

This work is supported by the National Natural Science Foundation of China (Nos. 61422404 and 51472219), Central basic scientific research in colleges and universities operating expenses, Program for Innovative Research Team in University of Ministry of Education of China (IRT13R54), State Key Laboratory of Optoelectronic Materials and Technologies (Sun Yatsen Unversity) and Zhejiang University K.P.Chao's High Technology Development Foundation.

References:

1. Y. Jia, J. Wei, K. Wang, A. Cao, Q. Shu, X. Gui, Y. Zhu, D. Zhuang, G. Zhang and B. Ma, *Adv Mater*, 2008, **20**, 4594-4598.
2. D. D. Tune, B. S. Flavel, R. Krupke and J. G. Shapter, *Advanced Energy Materials*, 2012, **2**, 1043-1055.
3. J. Wei, Y. Jia, Q. Shu, Z. Gu, K. Wang, D. Zhuang, G. Zhang, Z. Wang, J. Luo, A. Cao and D. Wu, *Nano Lett*, 2007, **7**, 2317-2321.
4. X. Li, Y. Jung, K. Sakimoto, T.-H. Goh, M. A. Reed and A. D. Taylor, *Energy & Environmental Science*, 2013, **6**, 879.
5. A. Ferrari, J. Meyer, V. Scardaci, C. Casiraghi, M. Lazzeri, F. Mauri, S. Piscanec, D. Jiang, K. Novoselov and S. Roth, *Phys Rev Lett*, 2006, **97**, 187401.
6. A. K. Geim and K. S. Novoselov, *Nature materials*, 2007, **6**, 183-191.
7. Y. Zhang, Y.-W. Tan, H. L. Stormer and P. Kim, *Nature*, 2005, **438**, 201-204.
8. K. Novoselov, A. K. Geim, S. Morozov, D. Jiang, M. K. I. Grigorieva, S. Dubonos and A. Firsov, *Nature*, 2005, **438**, 197-200.
9. X. Li, H. Zhu, K. Wang, A. Cao, J. Wei, C. Li, Y. Jia, Z. Li, X. Li and D. Wu, *Adv Mater*, 2010, **22**, 2743-2748.
10. E. Shi, H. Li, L. Yang, L. Zhang, Z. Li, P. Li, Y. Shang, S. Wu, X. Li, J. Wei, K. Wang, H. Zhu, D. Wu, Y. Fang and A. Cao, *Nano Lett*, 2013, **13**, 1776-1781.
11. L. F. Yang, X. G. Yu, M. S. Xu, H. Z. Chen and D. R. Yang, *Journal of Materials Chemistry A*, 2014, **2**, 16877-16883.
12. X. Li, W. Cai, J. An, S. Kim, J. Nah, D. Yang, R. Piner, A. Velamakanni, I. Jung, E. Tutuc, S. K. Banerjee, L. Colombo and R. S. Ruoff, *Science*, 2009, **324**, 1312-1314.
13. H. M. Branz, V. E. Yost, S. Ward, K. M. Jones, B. To and P. Stradins, *Appl Phys Lett*, 2009, **94**, 231121.
14. Y.-F. Huang, S. Chattopadhyay, Y.-J. Jen, C.-Y. Peng, T.-A. Liu, Y.-K. Hsu, C.-L. Pan, H.-C. Lo, C.-H. Hsu and Y.-H. Chang, *Nature nanotechnology*, 2007, **2**, 770-774.
15. A. Tataroğlu and Ş. Altındal, *Microelectron Eng*, 2008, **85**, 233-237.
16. Y. Zhang, W. Cui, Y. Zhu, F. Zu, L. Liao, S.-T. Lee and B. Sun, *Energy Environ. Sci.*, 2014.
17. G. K. Reeves and H. B. Harrison, *Electron Device Letters*, 1982, **3**, 111-113.
18. J. Britt and C. Ferekides, *Appl Phys Lett*, 1993, **62**, 2851.
19. B. Carr, E. Friedland and J. Malherbe, *J Appl Phys*, 1988, **64**, 4775-4777.
20. S. E. Shaheen, G. E. Jabbour, M. M. Morrell, Y. Kawabe, B. Kippelen, N. Peyghambarian, M. F. Nabor, R. Schlaf, E. A. Mash and N. R. Armstrong, *J Appl Phys*, 1998, **84**, 2324.
21. X. J. Wang, *J Appl Phys*, 2004, **95**, 3828.
22. T. M. Brown, R. H. Friend, I. S. Millard, D. J. Lacey, J. H. Burroughes and F. Cacialli, *Appl Phys Lett*, 2000, **77**, 3096.
23. T. Mori, H. Fujikawa, S. Tokito and Y. Taga, *Appl Phys Lett*, 1998, **73**, 2763-2765.
24. V. Mihailetchi, P. Blom, J. Hummelen and M. Rispens, *J Appl Phys*, 2003, **94**, 6849-6854.
25. C. J. Brabec, S. E. Shaheen, C. Winder, N. S. Sariciftci and P. Denk, *Appl Phys Lett*, 2002, **80**, 1288-1290.
26. E. Ahlswede, J. Hanisch and M. Powalla, *Appl Phys Lett*, 2007, **90**, 163504.
27. G. Li, C. W. Chu, V. Shrotriya, J. Huang and Y. Yang, *Appl Phys Lett*, 2006, **88**, 253503.

28. S. E. Shaheen, C. J. Brabec, N. S. Sariciftci, F. Padinger, T. Fromherz and J. C. Hummelen, *Appl Phys Lett*, 2001, **78**, 841.
29. Y. Zhang, R. Liu, S.-T. Lee and B. Sun, *Appl Phys Lett*, 2014, **104**, 083514.
30. Z. H. Ni, H. M. Wang, Z. Q. Luo, Y. Y. Wang, T. Yu, Y. H. Wu and Z. X. Shen, *J Raman Spectrosc*, 2009, **41**, 479-483.
31. S. Ryu, L. Liu, S. Berciaud, Y. J. Yu, H. Liu, P. Kim, G. W. Flynn and L. E. Brus, *Nano Lett*, 2010, **10**, 4944-4951.
32. L. Yang, X. Yu, W. Hu, X. Wu, Y. Zhao and D. Yang, *ACS Appl Mater Interfaces*, 2015, **7**, 4135-4141.

Table 1. Summary of photovoltaic parameters of devices with and without a LiF interlayer fabricated under the same condition.

Back electrode	V_{OC} (mV)	J_{SC} (mA/cm^2)	*FF* (%)	PCE (%)	R_s (Ω cm^2)
Al	336.21	25.63	44.21	3.81	2.43
	411.03	21.39	52.25	4.59	1.15
	361.55	26.59	45.18	4.34	0.95
	397.70	23.23	50.55	4.67	0.93
LiF/Al	424.83	27.11	54.23	6.25	0.85
	400.42	26.29	53.06	5.58	0.80
	405.34	24.83	54.50	5.48	0.92
	417.26	27.18	52.78	5.99	0.87

\

Figure captions

Figure 1. (a) Schematic diagram of a Gr-Si Schottky solar cell; (b) the Raman spectrum of a Gr film;

Figure 2. Scanning Electron Microscopy (SEM) image of 0.5 nm thick LiF layer deposited on Si.

Figure 3. (a) *J-V* curves under illumination of pristine and HNO_3 doped devices with and without a LiF interlayer; inset shows the photograph of device; (b) external quantum efficiency (EQE) spectra of devices with and without a LiF interlayer; (c) *J-V* curves of devices with or without a LiF interlayer under dark condition; (d) Series resistances (R_s) extracted from $dV/d(\ln J)$ versus *J* curves for our best Gr-Si Schottky junction solar cells with and without a LiF interlayer.

Figure 4. Contact resistance (R_c) extracted by the transmission line method (TLM) for the direct Al/Si contact and Al/LiF/Si contact. The inset shows the schematic picture of a device for measurements.

Figure 5. Scheme of band structure of devices (a) without and (b) with a LiF interlayer.

Figure S1. Schematic diagram for measuring the values of contact resistance of the Al/Si and Al/LiF/Si contact.

Figure S2. (a) *J-V* curves of Gr-Si solar cells with 0.5 and 1.2 nm thick LiF interlayers under illumination; (b) EQE spectrum of Gr-Si solar cells with 0.5 and 1.2 nm thick LiF interlayers

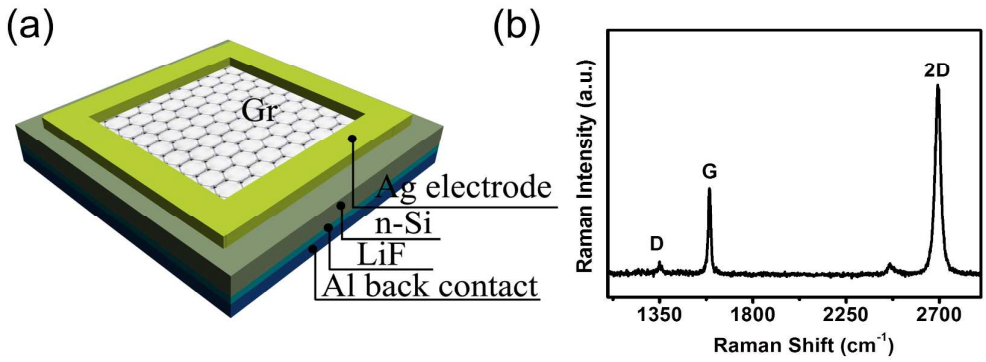

Figure. 1

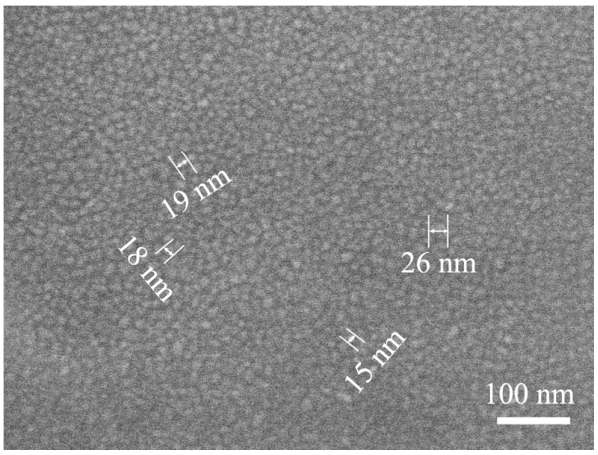

Figure 2.

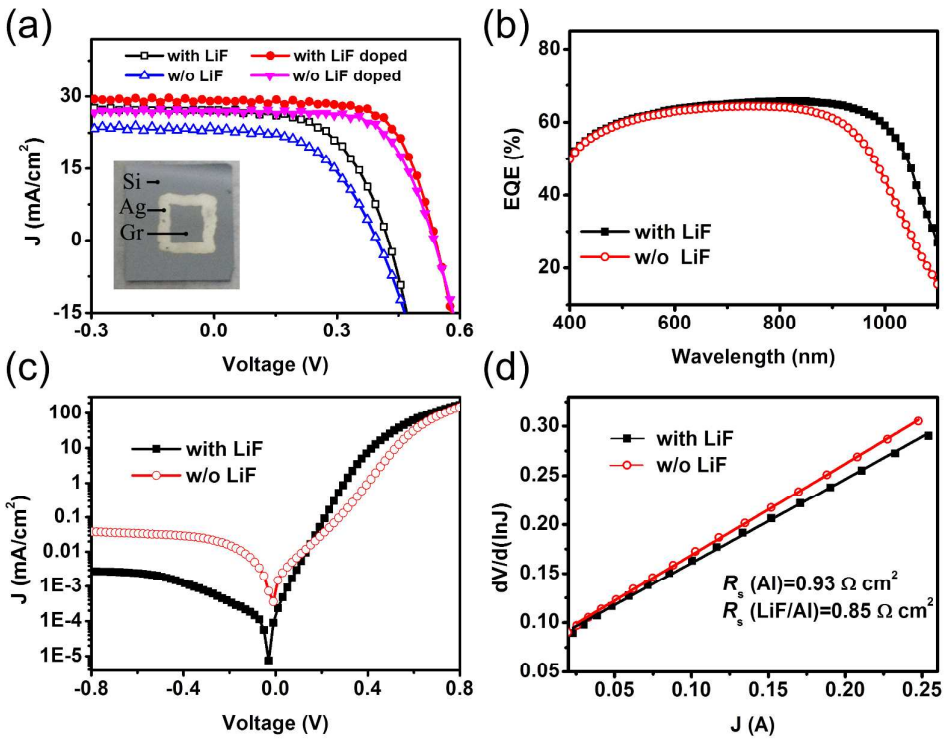

Figure. 3

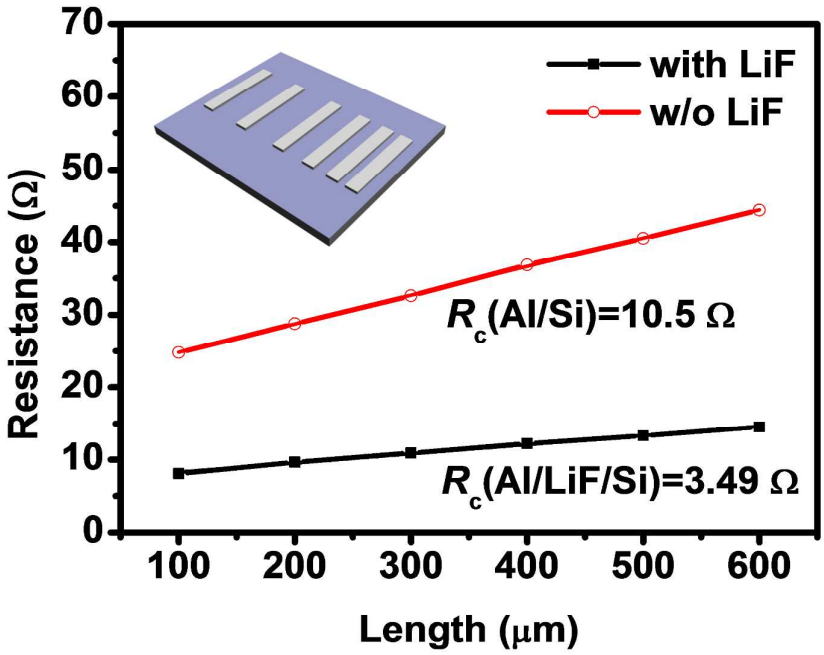

Figure. 4

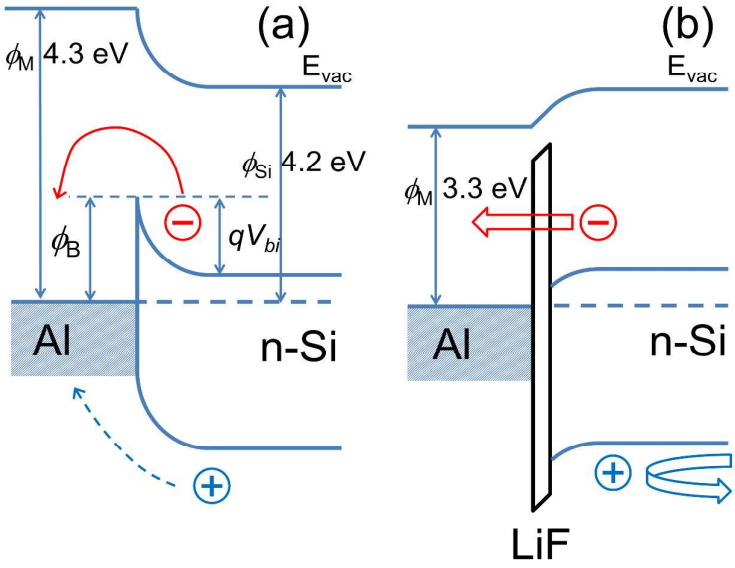

Figure. 5

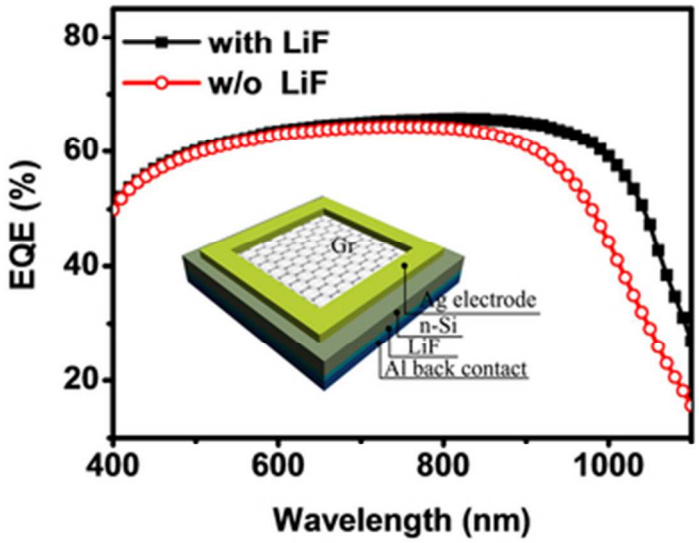

A thin LiF layer can suppress the back surface recombination and improve the efficiency of Gr-Si solar cells.

A thin LiF layer can suppress the back surface recombination and improve the efficiency of Gr-Si solar cells
39x29mm (300 x 300 DPI)